Road Maintenance Vehicles Location using DGPS, Map-Matching and Dead-Reckoning: Experimental Results of a Smoothed EKF

David Bétaille - *Laboratoire Central des Ponts et Chaussées - France*
Philippe Bonnifait - *Heudiasyc UMR 6599 - Université de Technologie de Compiègne - France*

BIOGRAPHY

David Bétaille is a junior researcher at the LCPC (the French public works research institute), and belongs to the Site Robotics subdivision. The main projects in which he participated are: CIRC, Computer Integrated Road Construction, a Brite-Euram project, for which he developed a simulator of a paver located by GPS; high-precision application of GPS in the field of real-time equipment positioning (97'IAARC congress best theory paper); and vehicles location using DGPS and dead-reckoning. He is also responsible of the localization systems tests facility of the LCPC, named SESSYL.

Philippe Bonnifait is an assistant professor at the Université de Technologie de Compiègne. His research activities concern non linear systems state estimation. The major application considered is the localization process of mobiles robots evolving outdoors on 3D surfaces. In 1997, he has participated to the Brite-Euram CIRC project for the development of the localization module of compactors. He is now with the Heudiasyc UMR 6599 and he works on driving assistance systems.

ABSTRACT

This paper presents a technique to localize outdoors vehicles equipped with a differential GPS receiver, an encoder attached to the wheels and a fiber optic gyrometer. As a precise location is not necessary in real-time for the application considered, the data of the sensors are stored on a computer, while the vehicle is moving, and fused afterwards. Different smoothing techniques are presented and discussed. Thanks to extensive real experiments with many masks of the satellites, a smoother has been validated in comparison with a Post-Processed Kinematic GPS. If the duration of the masks becomes too large, a method which uses a precise digital road map and a Geographical Information System is presented and validated with real data.

INTRODUCTION

In the fields of pavement management and road maintenance, dedicated vehicles investigate different properties of the road (surface, geometry...) with specially designed devices, based on various auscultation processes and on-board "auscultation sensors", using ultrasonic techniques. These monitoring vehicles patrol roads along itineraries which can be a hundred kilometers long. The measurements of the auscultation sensors are finally collected in databases where they are labeled using the distance from the nearer milestone.

For the road maintenance requirements, the specification concerning the precision of the location is one meter. Precision here means "repeatability" assuming that a patroller runs several times a given itinerary, collecting the different measurements. For each trial, a database is produced. One meter precision means that the standard deviation of the error on the distance label is around one meter.

For this purpose, the distance is measured using an on-board encoder, which is regularly corrected by manually captured event markers (milestones, crossroads...). In case of a higher patrolling speed or with different employees, this statistic would exceed one meter: a tricky problem is that the precision depends, firstly, on the way the operator captures the event markers and, secondly, on the state of the calibration of the on-board encoder.

On the other hand, Geographical Information Systems (GIS) appear to be well suited to pavement management. As the digital maps used by the GIS are defined with geographical coordinates, the use of GPS appears to be very appropriate. Moreover, a precision of one meter can be achieved in differential GPS (DGPS). Further, thanks to the corrections provided by geo-synchronous satellite DGPS services, receivers can achieve this precision over a wide area, suitable for the itineraries of the patrol vehicles. There is no need for a ground station and the precision is perfectly adapted to the problem considered.

Unfortunately, satellites are frequently obscured on roads because of trees, bridges, buildings, etc. In such situations, GPS cannot be used and the classical solution

consists in using inertial sensors like accelerometers, gyrometers or encoders attached to the wheels in order to provide a "precise enough" estimation of the position.

As the problem is to precisely localize the stored measurements of the auscultation sensors, the data of the "localization sensors" can be collected too and the localization process can be performed afterwards, when the mission is finished. The experimental results presented in the paper were obtained using a "KVH" fiber optic gyrometer, an odometer attached to the front driving wheels of the vehicle and a "Trimble Ag132" DGPS receiver associated with the "Landstar" corrections.

In this context, "non causal" operations can be applied to the stored measurements of the sensors. This means that these treatments are not feasible in real-time, because the data are filtered in the forward direction. For instance, the filtered results are reversed and run backwards through another filter.

In this paper, we present the effectiveness of different algorithms. In the first section, the sensors are presented. A dead-reckoning technique is then presented and tested. Section 3 gives the formalism of an Extended Kalman Filter (EKF) to fuse the encoder and gyro data, obtained at 10 Hz, and the DGPS locations (1 Hz). Two statistical smoothers are introduced in the following part and a geometrical method is presented, in section 5, to smooth the predicted locations between two DGPS points. If the satellites are obscured for a long time, the integration of the measurements of the inertial sensors will drift unboundedly. In this situation, we propose a method which uses a digital roadmap (section 6). Experimental results show the relevance of the methods studied and allows selection of the best smoother.

1. Localization sensors.

1.1. GPS.

GPS appears naturally very appropriate to provide the geographical coordinates [Abbott, Powell, 99] which are necessary to import the measurements of the auscultation sensors into a Geographical Information System (GIS).

Moreover, a precision of one meter can be achieved in differential GPS (DGPS). But several hundreds of kilometers must be covered by the road maintenance vehicles, during sessions of several hours. The use of a ground station transmitting its corrections by radio or telephone will cause a degradation of the precision and will introduce an evident problem of reliability.

Thanks to the corrections provided by geo-synchronous satellites like "Landstar" [Landstar, 2000] or "Omnistar" [Omnistar, 2000], DGPS receivers can achieve this precision over a wide area, suitable with the itineraries of the patrol vehicles. There is no need for a ground station and the precision is under one meter everywhere in the area covered, which is perfectly adapted to the problem considered.

The receiver we chose is a TRIMBLE Ag132 (GPS code on L1 frequency) running in DGPS by the differential correction service "Landstar". Ag132 tests performed on the SESSYL test bed in 1998 [Bétaille, 98] concluded that the 2D RMS obtained was 0.8 m. As these were carried out when the SA perturbation was on, we believe that the current precision is at least the same and almost certainly better.

Therefore, DGPS fits in with the requirement specifications except for the fact that it cannot be "continuous": masks of the satellites will cut off the signal, particularly in difficult environments like cities or forests. Dead-reckoning sensors are therefore needed.

1.2. Encoder.

An encoder (electro-mechanical shaft type generally) already exists on pavement management dedicated vehicles. At present, it provides the distance which is used as a label in road maintenance databases.

We have calibrated our encoder using a Post-Processed Kinematic GPS, in static mode, between two stations (situated on a straight line of length 1000 m) at which we stopped the vehicle. We estimate that the uncertainty of the calibration equals 1 "step" of the encoder per the performed distance, supposing that:

- the wheels do not slip,
- the rolling surface is perfectly planar,
- the PPK GPS location produces a negligible error.

Finally, the estimated step of the encoder is 121 mm, with an error of less than 1%.

In our algorithms, the distance measured by the existing encoder is effectively used and combined with other measurements. The encoder is one of the sensors used by a dead-reckoning technique when the DGPS does not work during masks. A gyrometer is the other one.

1.3. Gyrometer.

Practically, three main categories of gyrometers exist depending on the technique which is used [Barshan, Durrant-Whyte, 95]. These techniques are either piezo electric, fiber optic or mechanical. The current piezo electric devices are the less expensive devices and also the mode spread technique, particularly in Car Navigation Systems. They are ten times less expensive than fiber optic gyrometers, but not sufficiently precise for our application [Aubert, 97].

Fiber optic gyrometers measure the rotation speed or the heading, after an integration, by application of the "Sagnac effect" principle.

After a couple of tests [Bétaille, Bonnifait, 00], we have chosen a "KVH" fiber optic gyrometer (RD 2100 digital model) which outputs the heading rotation speed at the frequency of 10 Hz. Its performance (for a moderate price) appeared sufficient to meet our precision requirement.

The main technical characteristics of the KVH RD 2100 gyrometer are:

- amplitude: 100°/s
- resolution: 0.003°/s (16 bits signed)

At a constant temperature:

- angle random walk: 20(°/h)/√Hz
- bias repeatability: 0.02°/s
- non-linearity of the scale factor: 0.5% (full scale)

Temperature dependence of the specifications:

- bias variation vs temperature: 0.2°/s [-40°C;+75°C]
- scale factor variation vs temperature: 1%

In order to appreciate its performances, we performed two dynamic tests around the SESSYL track.

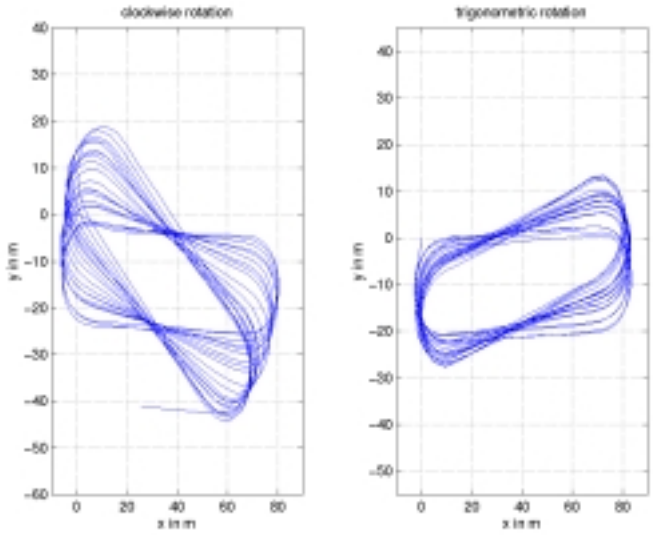

Fig.1: RD 2100 dynamic tests around the SESSYL track

The phenomenon of drift (around 1% after 20 revolutions) is illustrated by the results of the figure above. Since the temperature was stable, the bias has been identified once before each test. Here, we note that the sign of the drifts of the successive loops depends on the sign of the rotation around the track itself (the two experiments were performed in opposite directions). Since the maximum rotation speed is 30°/s, both non-linearity of the scale factor and dynamic effects (acceleration of the vehicle) probably explain the observed phenomenon.

1.4. Installation of the sensors in the testing vehicle.

The testing vehicle was a Peugeot J5 lorry, a kind of vehicle commonly used for road patrolling. The encoder measured directly the rotation of the gearbox, which is the mean of the rotation of the two front wheels on this vehicle. The gyrometer was horizontally fixed on the platform of the van. The GPS antennas (one for DGPS, the other for the Post-Processed Kinematic reference path provided by a TRIMBLE 4000 pair of receivers) were mounted on the roof with a known offset. The receivers were installed on-board.

1.5. Data collecting.

The following measurements:

- impulsions from the encoder,
- 10 Hz digital output of the gyrometer,
- GPS "pulse per second" output,

were collected on a PC by interrupts, and dated using a PC clock whose resolution was 0.01 s. The GPS pulse per second function of the TRIMBLE 4000 was used to synchronize the GPS time and the PC clock in the data fusion post-processing. The Ag132 was connected to another PC.

Thanks to this synchronization, the latency times of the GPS receivers have been compensated in the post-treatments.

2. Integration of the odometer and gyrometer data.

2.1. Kinematic model.

A simple kinematic model of the vehicle (1) was chosen. "x" and "y" are the coordinates of the vehicle, in a local reference frame, and θ its heading. The localized mobile frame is attached to the middle of the rear wheels of the vehicle.

We suppose that:

- the linear speed measured by the encoder is the one of the origin of the mobile frame,
- the trajectory is locally circular.

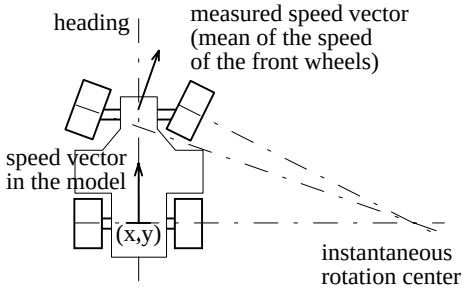

Fig.2: kinematic model

We then have the following discrete model [Bonnifait, Garcia, 98]:

$$\begin{aligned} x_{k+1} &= x_k + \Delta s.\cos(\theta_k + \Delta\theta/2) \\ y_{k+1} &= y_k + \Delta s.\sin(\theta_k + \Delta\theta/2) \\ \theta_{k+1} &= \theta_k + \Delta\theta \end{aligned} \qquad (1)$$

where Δs represents the variation of distance between two sampling instants and Δθ corresponds to the elementary variation of the heading. For the KVH gyrometer, Δθ=ω.Ts, where "Ts" represents the sample time and "ω" the measured heading rotation speed.

2.2. Experimental results.

The tests program contained 3 different tests repeated twice : 1st test (tests 1 and 1a), with no stop and no rotations except those of the circuit itself ; 2nd test (tests 2 and 2a), with no stop but with supplementary rotations like traffic circles ; 3rd test (tests 3 and 3a), with stops. The speed limit was 50 km/h.

A centimeter precision reference path was computed for each test, by PPK GPS. A pair of TRIMBLE 4000 receivers (GPS phases on L1 and L2 GPS frequencies for PPK) was used. The environment of the tests track guarantees excellent conditions to perform GPS measurements: there were no natural masks (they were in fact simulated in this study).

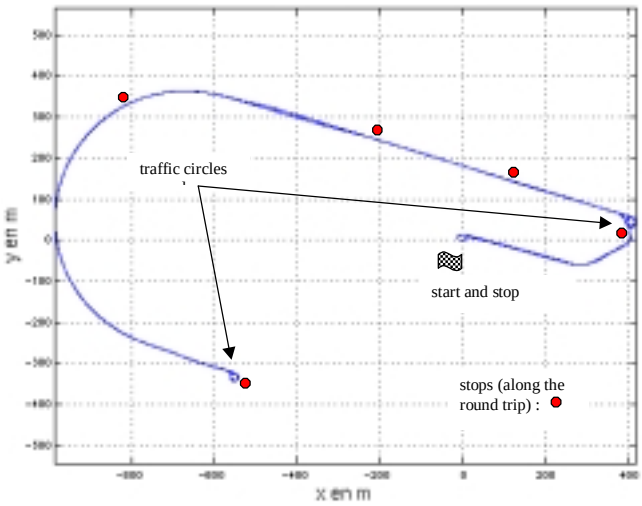

Fig.3: experimental path

The next figure represents the integration closing error of the dead-reckoning technique after completing the circuit. Despite different test conditions (traffic circles or stops) the closing error equals some tenths of meters.

The estimation shows a drift which is explained by:

- the approximation of the non-linear integration model,
- the fact that the road is not perfectly planar,
- the slipping of the wheels,
- the non-linearity of the gyro.

Considering these results, it is clear that the integration must be regularly corrected by independent measurements of position, which can be obtained by DGPS.

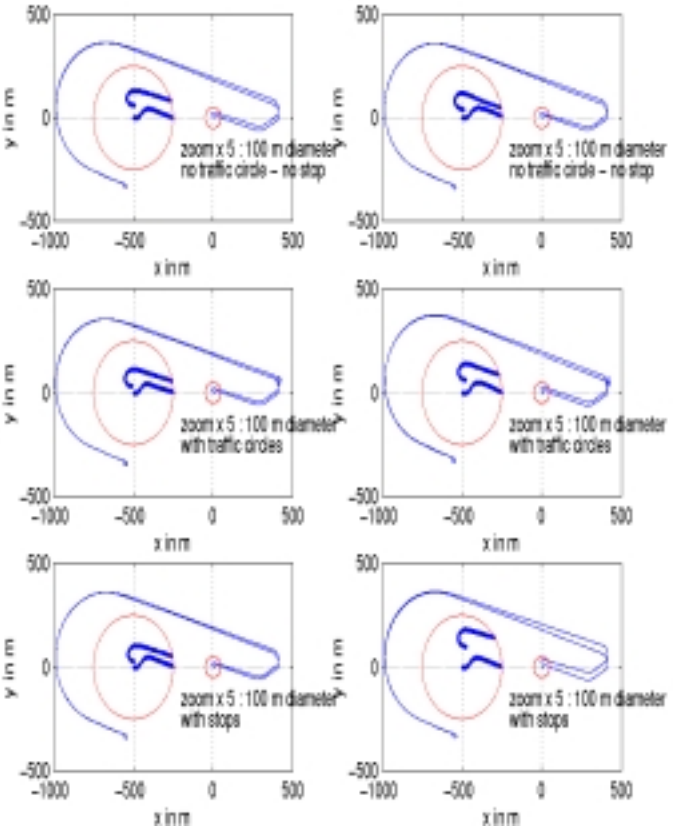

Fig.4: closing errors after completing the circuit

3. Integration of DGPS applying a Kalman real-time filter.

3.1. The extended Kalman filter.

An Extended Kalman Filter (EKF) can be applied to the measurements of the gyrometer and the odometer, using the DGPS locations as observations of the position. This formalism permits prediction of position even when the estimations by DGPS are not available.

There are two steps:

- successive predictions at 10 Hz,
- estimations by DGPS, at 1 Hz, if DGPS is available.

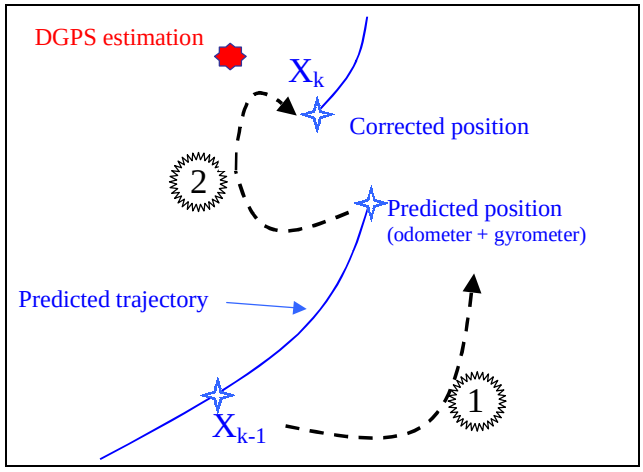

Fig.5: DGPS used to correct successive predictions

The formalism and the representation by matrices are well known, and can be found in the literature [Maybeck, 79].

The posture, X state vector, is classically defined as follows: position x and y, coordinates in a local reference frame, and θ, the heading of the vehicle:

$$X = \begin{bmatrix} x \\ y \\ \theta \end{bmatrix} \quad (2)$$

The input command vector, U, contains the variation of distance and the measurements of the gyrometer:

$$U = \begin{bmatrix} \Delta s \\ \omega * Ts \end{bmatrix} \quad (3)$$

The equations of the model are the same as we already displayed (1). The random phenomena are represented by centered and independent white noises, with known variances (α_k is the noise due to the model, which is tuned a posteriori):

$$X_{k+1} = f(X_k, U_k) + \alpha_k \quad (4)$$

Since those equations are non-linear, the formalism of Kalman is extended, developing (4) around the last estimation or prediction into a first order series of Taylor, which introduces Jacobian matrices [Chui, Chen, 91].

Further, let γ_k be the noise on the unknown input "U^*"; it includes the noise on the measure of the distance (its variance equals: step²/12) and the noise on the gyrometer, which is also tuned a posteriori:

$$U_k = U_k^* + \gamma_k \quad (5)$$

The equation of observation is linear. It uses "x_g" and "y_g", position output by DGPS (we suppose that the antenna is located on the vertical axis of the mobile frame); β_k is the observation noise, which bas been quantified by tests [Bétaille, 98]:

$$\begin{bmatrix} x_g \\ y_g \end{bmatrix} = \begin{pmatrix} 1 & 0 & 0 \\ 0 & 1 & 0 \end{pmatrix} * \begin{pmatrix} x \\ y \\ \theta \end{pmatrix} + \beta_k \quad (6)$$

$$\mathrm{var}(\beta_k) = 0.8^2\ \mathrm{m}^2 \quad (7)$$

The detailed equations of the EKF are not presented here but can be found in [Bonnifait, Garcia, 98]. The filter produces successive predictions of the position and heading using the model and the measured input vector, and in the same time, a computation of the variances on position and heading. When a DGPS measurement is available, the equation of observation is used, with a gain factor function of the variance-covariance matrix and the noise matrices.

3.2. Analysis of the results of the EKF.

The filter was applied on the registered data for every test. We simulated the obscured periods by suppressing the DGPS data for a series of masks of 60 s, separated by 10 s periods of available DGPS locations.

As the drift is never very important (thanks to DGPS estimations of the position), it is relevant to compute a comparison of paths (lateral deviations) between the filtered path and the reference path given by the 4000 PPK GPS receivers, as shown on the following figure.

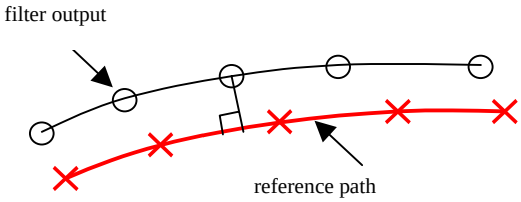

Fig.6: comparison of paths

Let's define the "2D RMS" as the square root of the sum of the squared lateral deviations.

Test n°	2D RMS (m)
1	2.5
1a	2.7
2	3.4
2a	2.8
3	1.9
3a	2.0

Frame 1: 2D RMS (EKF output path)

The noises for the model and the gyrometer were tuned so that the error between the filtered path and the reference path is always comprised into a 3σ envelop: σ is obtained with the variance EKF output matrices.

Even with the optimal tuning, the results are still far from the foreseen precision: one meter ! When a mask occurs somewhere the rotation speed is relatively important, an error of the predicted heading globally rotates the predicted path during the mask. Moreover, notice that the heading is not directly observed. When a mask occurs, the drift is due to the integration process but also due to the initial error on the heading.

Thereafter, we tested some of the non-causal filters which can be directly computed on the present results of the EKF because they use the same formalism.

4. Application of classical smoothers.

4.1. Forward and backward filtering technique.

In the backward technique, the EKF is processed from the end to the beginning, i.e. in decreasing time. Then, using the forward and backward filtered data, we compute an average path, using a weight proportional to the diagonal terms of the variance-covariance matrices.

Test n°	2D RMS (m)
1	1.5
1a	1.4
2	2.4
2a	2.2
3	1.1
3a	1.2

Frame 2: 2D RMS (averaging the EKF and the recursive EKF output paths)

Compared to the causal EKF (frame 1), this technique permits division by about 1.5 of the deviation between the path and its reference.

4.2. Rough's smoothing algorithm.

We also tested another smoother which uses the formalism of an EKF. It was designed by Rough and is commonly quoted [Labarrère, Krief, Gimonet, 93]: the method is also called: "maximum a posteriori" (MAP).

The MAP smoother on the complete test time interval (N) will be computed in two steps (see figure 7) :

- an EFK which computes and saves the predictions $\hat{x}_{k|k}$ and the variance covariance matrices $P_{k|k}$
- a recursive filter of the predictions, rewarding time, which delivers the smoothed values $\hat{x}_{k|N}$ and the variance covariance matrixes $P_{k|N}$

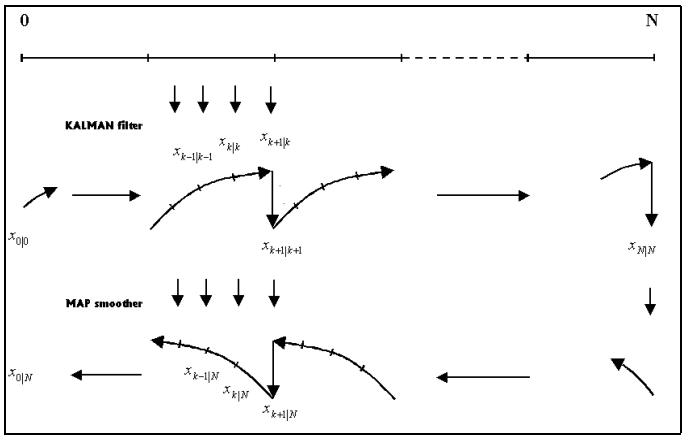

Fig.7: Rough algorithm

In this method, the smoothed value is equal to the (EKF) filtered value, plus a correction proportional to the deviation between the precedent smoothed value and the value predicted by the EKF.

$$\hat{x}_{k|N} = \hat{x}_{k|k} + C_k.\left(\hat{x}_{k+1|N} - \hat{x}_{k+1|k}\right) \qquad (8)$$

Test n°	2D RMS (m)
1	1.2
1a	1.2
2	1.5
2a	1.3
3	1.3
3a	1.3

Frame 3: 2D RMS (Rough output path)

The results are slightly better than the forward and backward filtering technique.

5. A geometrical smoother.

5.1. The geometric algorithm.

We observe that the main drawback of our filter is its inability to correct the heading in comparison with the position when an estimation is available. We have noticed that a simple rotation of the positions between two corrections significantly improves the precision, even when these corrections are separated by some tenths of seconds due to GPS masks.

In fact, this method has been used many times to modify globally a predicted path. If one starts and stops its circuit at known points, the method consists in calculating the geometric transformation in order to superpose the final predicted position with the position it should be in reality. This calculation is a similarity: a rotation with a scale factor.

In our problem, we suggest to repeat these rotation angle and scale factor transformations as many times as possible, i.e. each time a DGPS measurement is used to correct the dead-reckoning location (see figure 8).

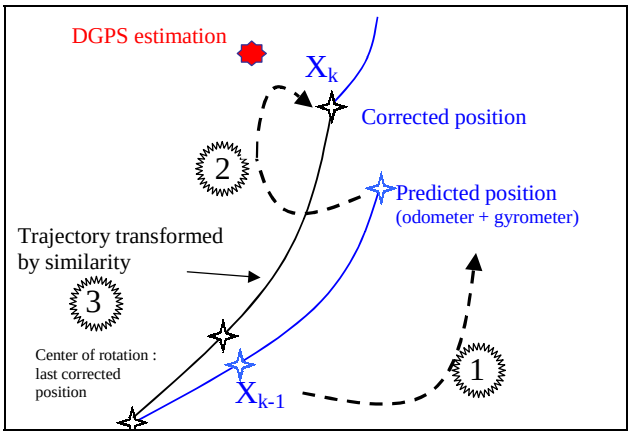

Fig.8: DGPS used to correct successive predictions

This has two advantages:

- it efficiently smoothes the "crab-wise" walking of the real-time filter,
- it produces adapted rotation angles and scale factors everywhere they can be calculated, and one can imagine easily that they will differ significantly from a linear portion of the circuit, compared to a strongly curved other portion.

Test n°	2D RMS (m)
1	1.4
1a	1.6
2	1.7
2a	1.6
3	1.3
3a	1.6

Frame 4: 2D RMS (similarity smoother output path)

This geometric method is not as efficient as the forward and backward EKF, or the Rough's MAP smoother. Nevertheless, the results here correspond to only the forward treatment. By now, we can also apply the same treatment backwards and combine the results.

5.2. Improving the geometric algorithm: rewarding time.

The geometric algorithm can be combined with the former forward and backward EKF. The combination should benefit from both:

- the ability of the recursive EKF to get the maximum precision in the extremities of obscured periods,
- and the ability of the similarity to reduce significantly the deviation in the middle of these periods.

We first compute the forward and backward paths, and store the diagonal terms of the variance-covariance matrices. Then, both paths are smoothed by similarity. Finally, the smoothed paths are combined using the weight proportional to the diagonal terms of the variance-covariance matrices.

Test n°	2D RMS (m)
1	0.9
1a	1.1
2	1.2
2a	1.3
3	0.9
3a	1.0

Frame 5: 2D RMS (similarity smoother output path, forward and backward averaged)

As expected, this combination of the smoothers gives the best results and approaches the level of precision demanded. The 2D RMS between the path and its reference has been divided by about 2.5.

6. Utilization of a GIS when long GPS masks occur.

The new geographical databases can reach nowadays a precision of a meter. Hence, when a long GPS mask occurs, the drift of the dead-reckoning can be corrected using a Geographical Information System.

In this situation, we propose the following method:

1. to compute a prediction phase using the encoder and the gyro,
2. to look for the nearest point on the road map,
3. to correct the prediction using a Kalman formalism.

This method is illustrated by the figure 9.

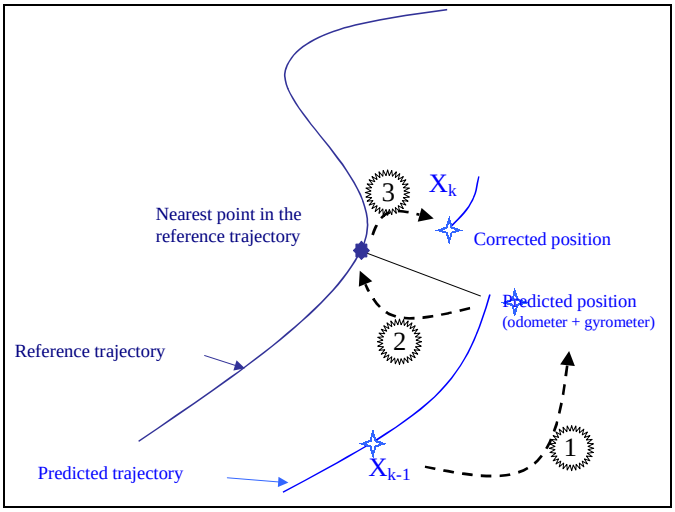

Fig.9: utilization of the map to correct successive predictions

This algorithm is done for all the inertial measurements (10 Hz) and is original in the way that the errors of the map are taken into account.

The observation equation which uses the nearest point (x_{ref}, y_{ref}) on the road map is analogous to equation (6).

$$\begin{bmatrix} x_{ref} \\ y_{ref} \end{bmatrix} = \begin{pmatrix} 1 & 0 & 0 \\ 0 & 1 & 0 \end{pmatrix} * \begin{pmatrix} x \\ y \\ \theta \end{pmatrix} + \beta'_k \qquad (9)$$

The observation noise "β'_k" has a standard deviation estimated to 2 m.

The results of an experiment are given on the following figure. The maximum speed of the car was 80 km/h.

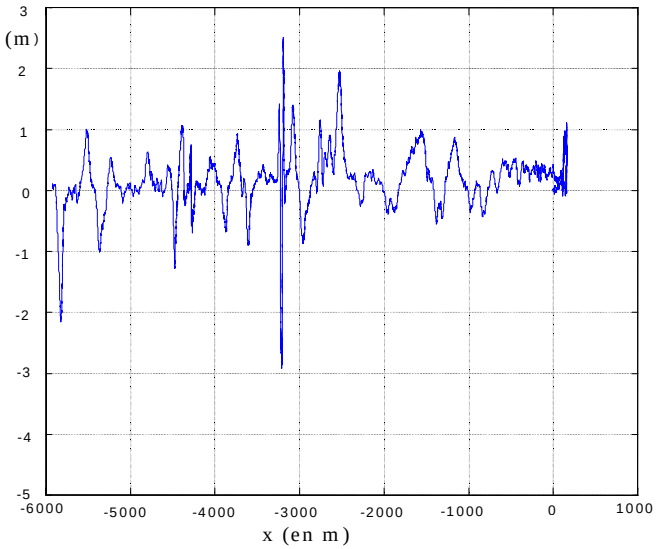

Fig.10: lateral deviation to the reference

The method gives good results since the maximum lateral deviation is 3 m for a trajectory of 6970 m long.

Nevertheless, the map-matching estimation phase does not allow a good correction of the longitudinal drift. As a matter of fact, we have noticed a longitudinal error of 18 m at the end of the trial, which corresponds to 0.26% of error. We think that this result is encouraging because it means that the longitudinal drift would be 1 m for a 300 m long mask, even with a high speed of the car.

CONCLUSION

The experimental results presented in the paper prove that precise localization of a vehicle, using a low-cost gyrometer, an odometer and DGPS is feasible. The attained precision is one meter, despite a series of masks which we consider to be particularly restricting. For long masks, the use of a GIS can provide sufficient accuracy of positioning.

Unfortunately, we have not tested our algorithms in urban environments for the reason that the kinematic GPS we use as a reference cannot reliably solve the ambiguity problem in such perturbed conditions. Tests should be done again, comparing the results of the package of sensors we chose with a high quality inertial navigation system (like military vehicles sometimes can be equipped). Another possibility could be to test our sensors on-board a railway wagon, or better an urban tramway, whose paths are repeatable and known with a couple of centimeters precision. Moreover, in all the experiments we have performed, the conditions of temperature were quasi identical. Hence, we did not evaluate any model to correct the KVH sensitivity to variations of temperature.

At the present time, drivers or supporters in patrolling vehicles have to capture the milestones and the crossroads along the itinerary, otherwise the error generated by the encoder cannot be corrected. The system presented could be used to replace the event markers, and as a consequence improve the security of drivers, supporters and other persons in the traffic. The quality of measurements can also be improved, because the attention was focused on the event markers instead of on the measurements themselves.

Finally the vehicle and the measurements of the auscultation sensors are able to be geographically referenced thanks to GPS, and as a consequence they can be directly exported in a GIS, satisfying the requirement of the final clients: road managers, political authorities...

ACKNOWLEDGEMENTS

The authors would like to thank the persons who participate in the experimental tests here mentioned, particularly the technical team (C. Lemaire, J.M. Prual, and F. Peyret for his assistance) and the students of the Ecole Centrale de Nantes (F. Aubert and P. Brochot).

REFERENCES

[Aubert, 97]: F. Aubert. "Localisation de mesures routières". Technical report. Ecole Centrale de Nantes. June 97.

[Abbott, Powell, 99]: E. Abbott and D. Powell. "Land-Vehicle Navigation using GPS". Proceeding of the IEEE, Vol. 87, NO. 1, January 1999].

[Barshan, Durrant-Whyte, 95]: B. Barshan et H.F. Durrant-Whyte. "Inertial navigation systems for mobile robots". IEEE Transactions on Robotics and Automation. Vol. 11, n°3, June 1995. pp. 328-342.

[Bétaille, 98]: D. Bétaille: "Ag132 – Rapport d'essais SESSYL", LCPC, 1998.

[Bétaille, Bonnifait, 00]: D Bétaille and Ph. Bonnifait. "Localisation de véhicules d'auscultation de routes avec l'utilisation de capteurs proprioceptifs, d'un récepteur DGPS, ou de données cartographiques". Journées GPS 2000. LCPC. 20-21 juin 2000. Nantes. France.

[Bonnifait, Garcia, 98]: Ph. Bonnifait and G. Garcia : "Design and Experimental Validation of an Odometric and Goniometric Localization System for Outdoor Robot Vehicles". IEEE Transactions on Robotics and Automation. Vol. 14, NO. 4, August 1998, pp. 541 - 548.

[Chui, Chen, 91]: C.K. Chui, G. Chen: "Kalman filtering with real-time applications", second edition, Springer Verlag, 1991.

[Labarrère, Krief, Gimonet, 93]: M. Labarrère, J.P. Krief, B. Gimonet: "Le filtrage et ses applications", Cépaduès editions, troisième édition, 1993.

[Landstar, 2000]: web site, http://www.landstar.com/

[Maybeck, 79]: P.S. Maybeck: "The Kalman filter: an introduction to concepts", Academic Press, Stochastic models estimation and control, Vol 1, pp. 3-16, 1979.

[Omnistar, 2000]: web site, http://www.omnistar.com/